Article:

Huang, H., Wang, C. and Chang, W. orcid.org/0000-0002-2218-001X (2021) Reducing human-induced vibration of cross-laminated timber floor - application of multi-tuned mass damper system. Structural Control and Health Monitoring, 28 (2). e2656. ISSN 1545-2255

https://doi.org/10.1002/stc.2656

Reducing human-induced vibration of cross laminated timber floor - Application of multi-TMD system

Haoyu Huang[a], Chang Wang[a], Wen-Shao Chang[b,*]

[a] Beijing Key Lab of Earthquake Engineering and Structural Retrofit, the Key Laboratory of Urban Security and Disaster Engineering of Ministry of Education, Beijing University of Technology, Beijing 100124, China

[b] School of Architecture, University of Sheffield, Sheffield S102TN, UK

[*] Corresponding author, w.chang@sheffield.ac.uk

Abstract

As a vibration control technique, tuned mass damper (TMD) system has been shown to be effective in reducing the human-induced vibration of a cross laminated timber (CLT) floor. However, the light-weight property of such a floor means there could be off-tuning when its mass varies. This study therefore developed a steel-based multi-TMD (MTMD) system and a shape memory alloy (SMA)-based MTMD system to reduce human-induced vibration of the CLT floor. Two 3-TMD systems in different locations and 5-TMD systems were designed to be effective within a certain bandwidth. The results show that SMA-based 5-TMDs are the most effective in reducing human-induced vibration, e.g., single-person and two-person slow walking, fast walking, and running, as they can cover a wider frequency band. By contrast, the effectiveness of the steel-based MTMD systems was unsatisfactory owing to permanent deformation of the steel components. When the loads on the CLT floor changed, the SMA-based 5-TMDs exhibited high robustness and was able to maintain the response at a low level. Test results show that a high-frequency excitation could degrade the effectiveness of the MTMD, as this is beyond the effective bandwidth. Therefore, future investigations should focus on developing strategies to enlarge the bandwidth of the MTMD.

Keywords: Cross laminated timber floor, Shape memory alloy, Multiple tuned mass damper, Human-induced vibration

1. Introduction

As a low-carbon construction material, timber has become increasingly popular in modern building projects. The rapid development of timber engineering is primarily due to the deep processing technology involved, a typical example of which is cross laminated timber (CLT). Existing practices show that the serviceability of the CLT floor should be considered more closely than that of floors using traditional construction materials.

In most design methods for floors [1-3], static deflection is a key criterion. In Eurocode 5, a frequency criterion known as the 8 Hz limitation is set for timber floor design. However, CLT structural design is not included in Eurocode 5. To meet the serviceability requirement, CLT floors with a larger thickness are often employed, which can cause material waste and nullifies the construction expediency advantage of CLT. With the development of vibration control techniques, employing a tuned mass damper (TMD) has been shown to be an effective way to reduce floor vibration [4-9]. By applying TMD, Webster and Vaicaitis [5] and Nguyen et al. [8] successfully reduced the human-induced vibration of concrete floor systems by approximately 60% and 40%, respectively. Wang et al. [10] proposed a general vibration control methodology for floor vibration using TMD system, and the results showed the optimised TMD system plays an important role in reducing the floor vibration. In theoretical terms, the TMD consists of mass m, stiffness k and damping c, which function to resonate with the main structure and further dissipate the energy.

However, a drawback of TMD is off-tuning as the mass on the CLT floor is not fixed. A change in configuration or use of the structure could cause the natural frequency of the system to shift, as a result of which the vibration could be greatly amplified. Timber is a light-weight material, and research has shown that it is easier to encounter the off-tuning problem in a CLT floor with TMD by changing the floor weight [11]. The semi-active TMD is a passive vibration control system with adjustable parameters. This can retune the primary structure in order to control the structural response [12, 13]. Our previous studies developed a shape memory alloy (SMA)-based temperature-controlled semi-active TMD for CLT floors, which effectively reduces the vibration caused by off-tuning [11, 14]. Another solution for off-tuning is to apply a multiple TMD system, which means that more than one TMD is installed on the floor. A MTMD system covers a wider frequency band and is less sensitive to the uncertainties of the floor [15]. The MTMD has been shown to be more effective than the standard TMD, the dynamic mechanics of which is presented in a previous study [16]. The effectiveness and robustness of MTMD were designed and evaluated by Dehghan-Niri et al. [17]. Semi-active methods such as temperature control

[11, 14], magnetorheological control [18], and SAVIS-TMD control [19] require energy supply, complex mechanical operation, and computer control algorithms, which increases the difficulties and uncertainties surrounding long-term civil engineering applications. The MTMD system is passive-control and is more robust for massive vibration excitations such as human-induced vibration of the floor [8, 20]. Therefore, it is important to carry out research on the application of MTMD to the CLT floor to reduce vibration.

In the previous study, SMA was applied to the TMD system on a CLT floor [11, 14]. SMA is a smart material and has a phase transformation property, as shown in Figure 1 (a). There are four phase transformation temperatures, M_s, M_f, A_s and A_f, which indicate the start and finish temperatures of the martensitic and austenitic transformations, respectively. Two unique mechanical characteristics of SMAs are superelasticity (Figure 1 (b)) and the shape memory effect (SME) (Figure 1 (c)) [21]. The stress-strain curve of superelasticity reveals that the recoverable strain is large because the SMA can virtually return to its original shape, even though the curve passes the yield point and nonlinear deformation occurs. Our previous study performed material characterisation on NiTi and Cu-Al-Mn SMA bars under dynamic bending. The results showed that superelastic SMA had a long fatigue life, stable hysteresis, and a large damping ratio during dynamic loading [22]. However, the dynamic properties of traditional construction materials such as steel can be greatly affected by the residual strain in plastic deformation, and there is no damping in elastic deformation. SMA has the potential to be employed in the TMD system for the floor. The performance of the superelastic SMA in structural control can also be found in [23]. It is therefore important to compare the effectiveness of a steel-based MTMD with a SMA-based TMD.

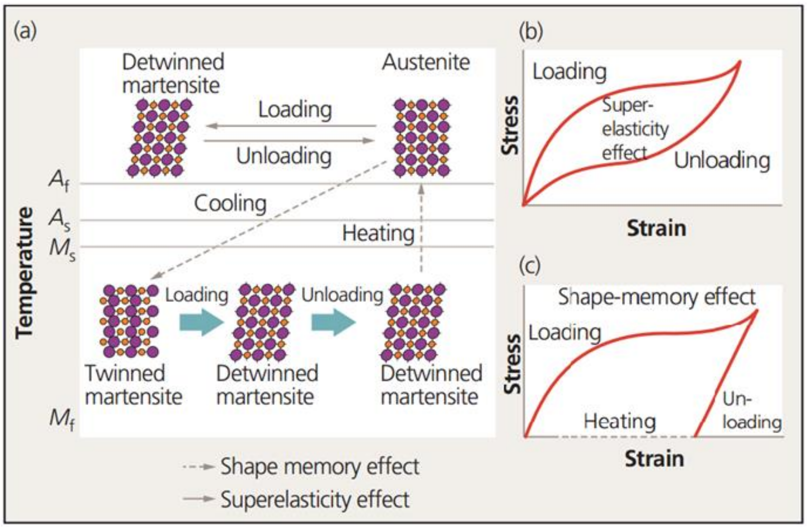

Figure 1 (a) Different phases of SMAs at various temperatures and a stress-strain curve demonstrating (b) superelasticity and (c) the shape memory effect [24]

In this study, different arrangements of steel-based and SMA-based MTMD systems were employed in a CLT floor for the reduction of human-induced vibration. It comprised a series of experimental tests conducted on a full-scale one-way CLT floor supported by steel beams. Slow walking, fast walking, and running loads exerted by one person and two people were the inputs used to assess effectiveness in serviceability. A single-TMD system was tested in the same scenario as a reference. The aim was to optimise the effectiveness of TMD control on a CLT floor and investigate how robustness of the MTMD system can be achieved in the application.

2. Fabrication of the CLT floor system and its dynamic properties

Figure 2 presents the CLT floor arrangement in the testing condition. The CLT floor was 6 m in span and 5.6 m wide. It was joined by five CLT panels with dimensions of 6×1.2 m using half-lapped joints. The 3-Ply CLT panels of 105 mm thickness were provided by Sino-Canada Low-Carbon Ltd, and the raw material was hemlock spruce (Tsuga chinensis). The moisture content of the timber was 12% tested in a storage condition of 40% R.H. 10℃. The material characteristics of CLT are tabulated in Table 1. The CLT floor spanned one way and was supported by two I beams, the construction details of which are presented in Table 2. The CLT floor was connected to the top flange of the steel beams by drilling self-tapping screws from the bottom up. The fabrication details of the column and column-beam connections are presented in Figure 3. To ensure its integrity and prevent the column from rocking, the column footings were connected using four steel beams.

Table 1 The material characteristics of the CLT

Density ($\boldsymbol{kg/m^3}$)	500
The modulus of elasticity parallel to grain (MPa)	5.45
The modulus of elasticity perpendicular to grain (MPa)	2020

Table 2 Fabrication details of the steel I beams

Category	HN450×200 (specified in the standard of GB/T 11263-2017 **[25]**)
Grade of the steel	Q235 (specified in the standard of GB/T 700-2006 [26])

Figure 2 CLT floor system used in experimental testing

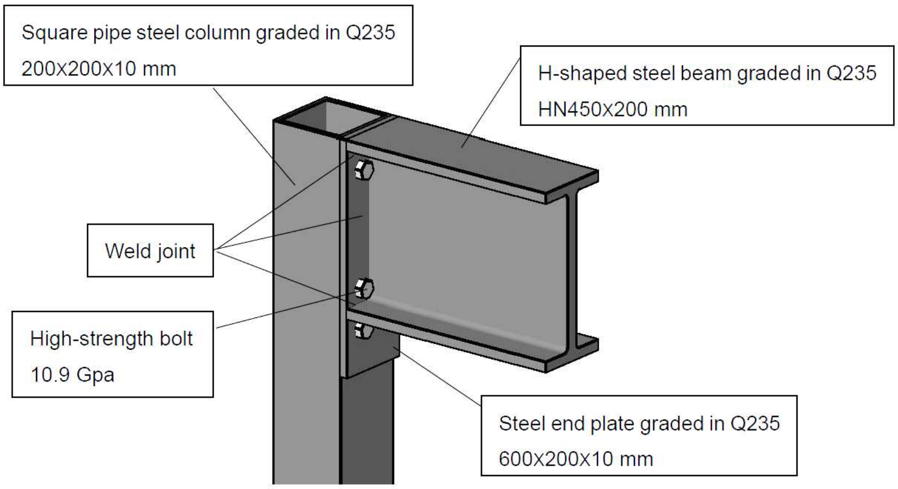

Figure 3 Fabrication details of the beam-column connections

As shown in Figure 4 (a), an accelerometer was installed on the central point on the floor, and the sampling rate was 1000 Hz. On the top of the CLT floor (Figure 2), sandbags weighing 0.08, 0.35, 0.50, 0.65 and 1.50 tons were placed to simulate the permanent actions of 0.02, 0.11, 0.15, 0.19 and 0.45 kN/m^2, respectively. The modal analysis was carried out using heel-drop tests conducted by a person of mass 75 kg, as shown in Figure 4 (b). Dynamic parameters such as natural frequencies, damping ratio, and modal masses were analysed from the measured acceleration. The analytical methods for the dynamic parameters were based on a linear-prediction singular-value decomposition-based matrix pencil (SVD-MP) method, detailed descriptions of which can be found in Sarkar and Pereira [27] and Zieliński and Duda [28]. The dynamic properties of the CLT floor under different loads are presented in Table 3. These show that the natural frequency decreases as the loads increase. The damping ratio is also larger when there are larger loads on the floor. The reason for employing the SVD-MP method is that it exhibits high precision when estimating the frequencies and damping ratio from the measured data. The spectra in frequency domain analysed by FFT under a load of 0.50 t is presented in Figure 5. This clearly shows there are two peaks at 5.21 and 8.42 Hz, which means that the vibration is dominated by the first mode shape and the second mode shape. Mode shapes under the load of 0.50 t are shown in Figure 6. The first mode shape is that of longitudinal bending (Figure 6 (a)), the second mode shape is a torsion about the longitudinal axis (Figure 6 (b)), and the third mode shape is that of transversal bending (Figure 6 (c)).

(a)

(b)

Figure 4 (a) Installation of the accelerometer; (b) Heel-drop tests

Table 3 The dynamic properties of the CLT floor under different dead loadings

Total loads on the floor (ton)	0.08	0.35	0.50	0.65	1.50
Fundamental natural frequency (Hz)	5.45	5.24	5.21	5.07	4.62
Mass (kg)	2020	2290	2444	2590	3440
Damping ratio (%)	1.32	1.93	2.14	2.65	2.08

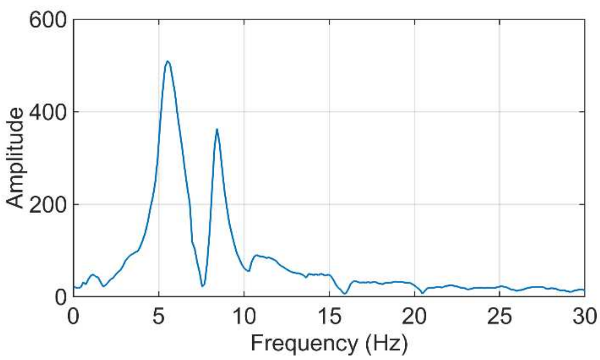

Figure 5 The spectra in frequency domain analysed by FFT under a load of 0.50 t

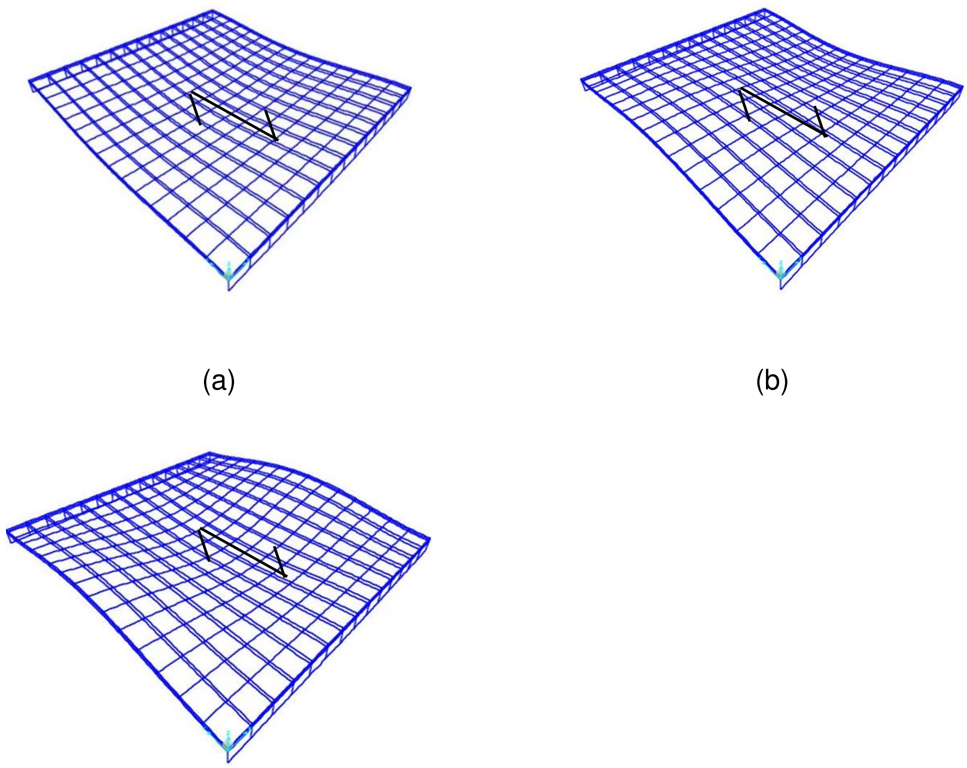

(a) (b)

(c)

Figure 6 (a) First mode shape of the CLT floor (corresponding frequency: 5.21 Hz); (b) Second mode shape of the CLT floor (corresponding frequency: 8.33 Hz); (c) Third mode shape of the CLT floor (corresponding frequency: 10.83 Hz)

3. Design and fabrication of the MTMD system

Both steel-based MTMD and SMA-based MTMD were investigated in identical testing conditions. This is because the main material in MTMD is mobile and can be switched to steel or SMA. The configuration of the single TMD in this study employed the TMD design used in our pilot study [11]. One of the MTMD systems is shown in Figure 7 (a). Its installation is presented in Figure 7 (b). Two masses were symmetrically cantilevered on a steel support, and the connecting bar between the steel support and the attached mass was made of steel or SMA so that the steel/SMA bar could be bent to provide the stiffness and damping. The steel bar used in TMD is stainless steel graded in 304 as specified in the standard [29]. The SMA used in the TMD was Ni-Ti (Ni = 55.74%, Ti = 43.73%, and V = 0.53%) SMA, and the phase transformation temperature was approximately -30℃. This was tested using differential scanning calorimetry. This revealed that, in room temperature, Ni-Ti SMA exhibited superelasticity (Figure 1 (b)). The modulus of elasticity of Ni-Ti SMA is

83 GPa and its ultimate strength is 1050 MPa. A comprehensive material characterisation of Ni-Ti SMA was conducted in our previous material study [22], the results of which showed that the stiffness, damping capacity, and fatigue property of Ni-Ti SMA are reliable in terms of its dynamic application.

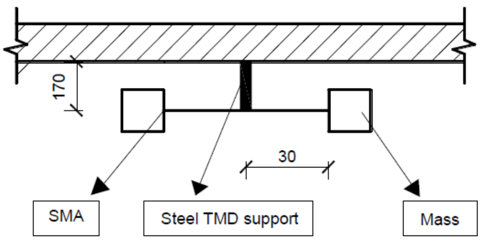

(a) (b)

Figure 7 (a) One of the SMA-based MTMDs installed on the CLT floor; (b) Drawings of the installation of the SMA-based MTMD

The optimal design of the TMD was first proposed by Den Hartog [30] as presented in Equations (1) and (2):

$$f_{opt} = \frac{1}{1+\mu} \tag{1}$$

$$\xi_{opt} = \sqrt{\frac{3u}{8(1+\mu)}} \tag{2}$$

where μ denotes the mass ratio between the TMD and the main structure. f_{opt} and ξ_{opt} denote the optimal frequency ratio and damping ratio, respectively. In Den Hartog [30]'s theory, the structure-TMD system is simplified to a 2-degree-of-freedom (DOF) system. Through the dynamic equation derivations of a 2-DOF system, reaching f_{opt} can facilitate resonance between the TMD and the main structure, while reaching ξ_{opt} can lower the amplitude at a wider frequency band. For the MTMD system applied to the CLT floor, the theoretical model could not be simplified to a 2-DOF system. A schematic diagram of the MTMD system is shown in Figure 8, in which a single-DOF structure is attached by n masses in parallel. m_s, k_s and c_s are the mass, stiffness, and damping coefficient of the CLT floor while m_n, k_n and c_n are the mass, stiffness, and damping coefficient of the n^{th} damper.

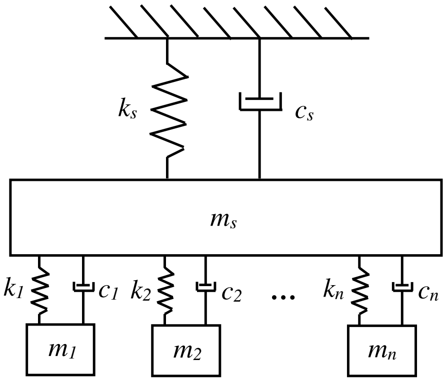

Figure 8 Schematic diagram of the MTMD system installed on the CLT floor

Under the excitation of a harmonic load $Pe^{i\omega t}$ to the main structure, the dynamic equations of the system are as shown in Equation (3):

$$
\begin{bmatrix} m_s & & & \\ & m_1 & & \\ & & \cdots & \\ & & & m_n \end{bmatrix}
\begin{bmatrix} \ddot{x}_s \\ \ddot{x}_1 \\ \cdots \\ \ddot{x}_n \end{bmatrix}
+
\begin{bmatrix} c_s + \sum_{j=1}^{n} c_j & -c_1 & & -c_n \\ -c_1 & c_1 & & \\ & & \cdots & \\ -c_n & & & c_n \end{bmatrix}
\begin{bmatrix} \dot{x}_s \\ \dot{x}_1 \\ \cdots \\ \dot{x}_n \end{bmatrix}
+
\begin{bmatrix} k_s + \sum_{j=1}^{n} k_j & -k_1 & & -k_n \\ -k_1 & k_1 & & \\ & & \cdots & \\ -k_n & & & k_n \end{bmatrix}
\begin{bmatrix} x_s \\ x_1 \\ \cdots \\ x_n \end{bmatrix}
=
\begin{bmatrix} Pe^{iwt} \\ 0 \\ \cdots \\ 0 \end{bmatrix}
\quad (3)
$$

Following simplification, Wang and Shi [31] proposed an optimal design method for MTMD system based on Den Hartog [30]'s methods. The detailed derivation process is described in [27]. The design process for the MTMD system is presented in the flow chart in Figure 9. Firstly, the number of TMDs (n) and the mass ratio (μ) are selected. It is important to note that μ is a ratio between the total mass of the TMDs and the main structural mass. The central frequency ratio of the MTMD is then set to 1 in accordance with the suggestion in [27]. The next step is to ensure the MTMD can tune in a bandwidth rather than a single frequency. By calculating Equations (4) and (5), the optimal frequency bandwith (χ_{opt}) and the optimal TMD damping ratio (ξ_{opt}) can be acquired.

$$\chi_{opt} = 1.048 - \frac{0.498}{\ln(n)} + 0.27\ln(\mu) + \frac{0.108}{[\ln(n)]^2} + 0.02[\ln(\mu)]^2 - \frac{0.05\ln(\mu)}{\ln(n)} \quad (4)$$

$$\xi_{opt} = 0.175 + \frac{0.092}{n} + 0.058\ln(\mu) + \frac{0.074}{n^2} + 0.005[\ln(\mu)]^2 + 0.019\frac{\ln(\mu)}{n} \quad (5)$$

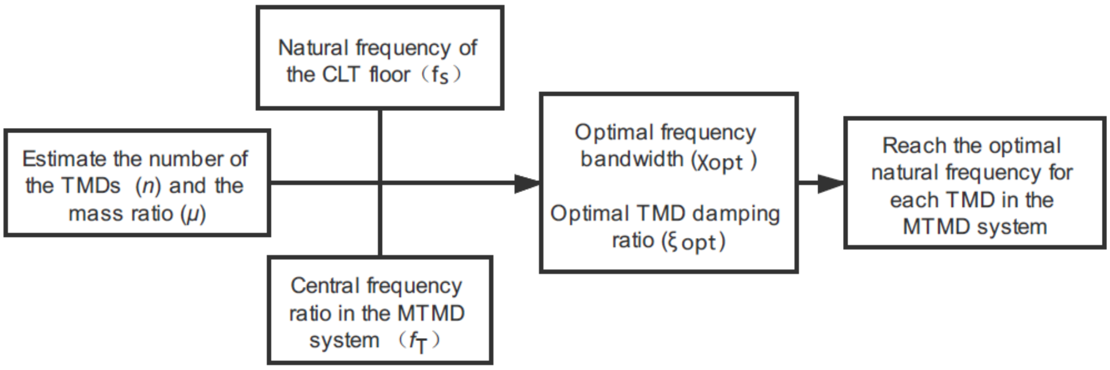

Figure 9 Design process for the MTMD system

In this study, MTMD systems with TMDs (n) of 3 and 5 were selected and named "3-TMDs" and "5-TMDs", respectively. The optimal design was based on a CLT floor under a load of 0.50 t. The calculations for χ_{opt} and ξ_{opt} for steel-based 3-TMDs and 5-TMDs using Equations (4) and (5) are shown in Table 4. The fundamental natural frequency and damping ratio of each TMD in the MTMD were calculated using χ_{opt} and ξ_{opt} in accordance with the methods in Figure 9. The parameters of the steel-based 3-TMDs and 5-TMDs applied to the CLT floor are shown in the 2nd-4th columns of Table 5. In this study, the damping ratio was not optimally designed and the vibration control was based on frequency tuning.

To make a compariosn, the steel bars were replaced by the SMA bars to conduct the tests in the same scenario. To compare the effect of different materials on the MTMD, the tuning bandwidth of the MTMD was kept constant in both testing programmes. Therefore, due to the lower stiffness of the SMA, each SMA-based TMD was designed to have a smaller attached mass in turn, as shown in the 5th-7th columns of Table 5. However, there was an error of approximately 10% between the actual and optimal tuning bandwidth when the SMA bars were applied. The damping ratio of the SMA-based MTMD was also not optimal.

Table 4 Results for χ_{opt} and ξ_{opt} for the steel-based 3-TMDs and 5-TMDs

	3-TMDs	5-TMDs
μ	0.027	0.044
χ_{opt}	0.144	0.181
ξ_{opt}	0.034	0.039

Table 5 Parameters of the 3-TMDs and the 5-TMDs

MTMD type	Steel-based MTMD Fundamental natural frequency (Hz)	Steel-based MTMD Mass (kg)	Steel-based MTMD Damping ratio (%)	SMA-based MTMD Fundamental natural frequency (Hz)	SMA-based MTMD Mass (kg)	SMA-based MTMD Damping ratio (%)
3-TMDs	4.83	24.60	0.14	4.83	13.20	0.14
	5.20	21.80	0.13	5.20	11.40	0.08
	5.57	18.34	0.14	5.57	9.44	0.14
5-TMDs	4.71	25.60	0.14	4.71	14.20	0.16
	4.96	24.00	0.13	4.96	12.20	0.12
	5.20	21.80	0.13	5.20	11.40	0.08
	5.45	19.46	0.14	5.45	10.40	0.13
	5.69	17.30	0.17	5.69	9.20	0.12

There were two location plans for the 3-TMDs, which were named “3-TMDs-a” and “3-TMDs-b”. The location arrangements for both are shown in Figures 10 (a) and (b), respectively. In both 3-TMDs-a and 3-TMDs-b, one of the TMDs was located at the central point with the maximum modal amplitude. In 3-TMDs-a, the TMDs were aligned in a transversal direction and two were placed near the edge of the floor. This tuned the second and third mode shapes of the CLT floor (Figures 6 (b) and (c)) to reduce the vibration caused by torsion and transversal bending. In 3-TMDs-b, the TMDs were aligned in a longitudinal direction and two were at the quarter span. The aim of this arrangement was to tune the first mode shape, which is longitudinal bending. As presented in Figure 10 (c), 5 TMDs were employed and named “5-TMDs”. In these, the arrangements of 3-TMDs-a and 3-TMDs-b were combined and thus the aim was to tune the first three mode shapes simultaneously. Figure 11 shows the instalment of the 5-TMDs on the tested CLT floor.

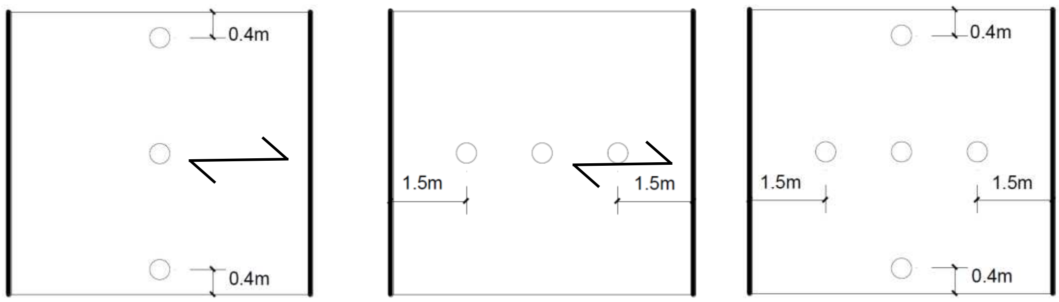

(a) (b) (c)

Figure 10 (a) 3-TMDs-a locations; (b) 3-TMDs-b locations; (c) 5-TMDs locations

Figure 11 Instalment of the 5-TMDs

4. Testing plan

The excitation considered in this study is human-induced vibration. In an area of 6×5.6 m in a residential house, there are likely to be one or two persons carrying out activities at the same time. Therefore, slow walking (1.27 Hz), fast walking (1.77 Hz), and running (2.22 Hz) by a single person and two persons were considered. The moving path of the testers was along a longitudinal direction from the midpoint of one edge to the midpoint of another, as shown in Figure 12 (a) and (b). The weight of the testers was between 60-70 kg. When two people were walking and running, the distance between them was approximately 0.5 m.

(a) (b)

Figure 12 (a) Single-person excitation; (b) Two-person excitation

The testing protocol is shown in Table 6. To set a reference, a non-TMD and single-TMD were compared with MTMD systems. The single-TMD was designed to have a fundamental natural frequency of 5.20 Hz, which is close to that of the CLT floor for a resonant effect. The single-TMD was installed on the central point of the floor. In tests Nos.

1-10, the effects of materials, number of TMDs, and locations of MTMD were studied. Because a CLT floor is light-weight, variation in structural mass also had to be considered. In Tests Nos. 11-50, the loads on the CLT floor were varied to cause off-tuning. Because MTMD can tune a number of frequencies, its robustness needed to be studied. There were six repetitions in each testing condition.

Table 6 Testing protocol

	Loads on the floor (t)					Materials used in MTMD	MTMD types
	0.50	0.08	0.35	0.65	1.50		
Test No.	1	11	21	31	41	Steel-based	Non-TMD
	2	12	22	32	42		Single-TMD
	3	13	23	33	43		3-TMDs-a
	4	14	24	34	44		3-TMDs-b
	5	15	25	35	45		5-TMDs
	6	16	26	36	46	SMA-based	Non-TMD
	7	17	27	37	47		Single-TMD
	8	18	28	38	48		3-TMDs-a
	9	19	29	39	49		3-TMDs-b
	10	20	30	40	50		5-TMDs

5. Results and discussion

5.1 Assessing the floor response: vibration dose value

Vibration dose value (VDV) is a popular method for evaluating floor response [32, 33]. It can be calculated as shown in Equation (6):

$$\mathrm{VDV} = \left[\int_0^T a_w^4(t)dt\right]^{\frac{1}{4}} \tag{6}$$

where $a_w(t)$ is the weighted acceleration and the frequency weighting spectra refers to BS 6472-1:2008 [32]. The weighting means that the acceleration data is filtered and amplified in a frequency range of 4-12.5 Hz. This assumes that a person is more sensitive within that particular range. The frequency-weighting curve for vertical vibration proposed in BS 6472-1:2008 [32] is presented in Figure 13. The comparison between raw time-history data and weighted time-history data can be found in [11]. T denotes the time during which the floor is excited. In this study, T was assumed to be the total time of each testing programme. VDV is widely applied in areas such as civil engineering, mechanical engineering, and vehicle engineering to control the vibration exposure limit for a person within a designated period of time.

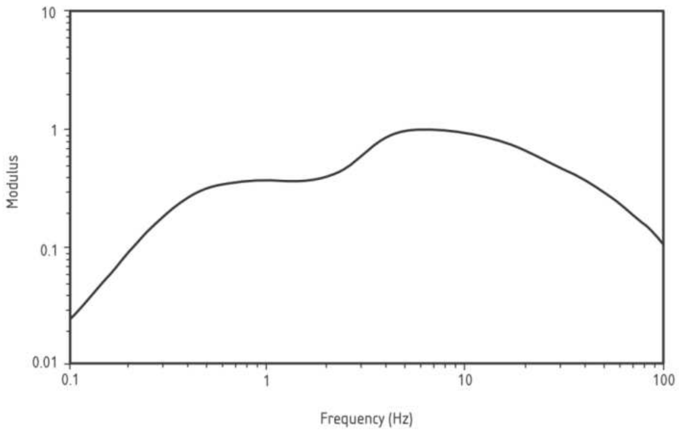

Figure 13 Frequency-weighting curve for vertical vibration proposed in BS 6472 [32]

5.2 SMA-based MTMD systems

Figure 14 (a) and (b) presents the VDV of the CLT floor in Tests Nos. 6-10. This shows that the VDV under running excitation has the largest value, followed by the VDVs under fast walking and slow walking. CLT floor responses under walking and running were reduced by applying the SMA-based MTMD system. As shown in Figure 14 (a), compared with the VDV of the CLT floor without TMD control, the VDV under single-person running equipped with SMA-based single-TMD, 3-TMDs-b, and 5-TMDs can be reduced from 1.614 $m/s^{1.75}$ to 1.173, 0.886, and 0.809 $m/s^{1.75}$, respectively. It is notable that 5-TMDs and 3-TMDs-b can reduce the VDV by approximately 50% and 45%, respectively in contrast to the non-TMD-controlled system. However, the reduction of VDV using a single-TMD is smaller at approximately 27%. As shown in Figure 15 (a), the time-history analysis of one event of single-person running shows that TMD is effective in decreasing the vibration amplitudes, especially after the first 3 seconds. In Figure 15 (b), the effectiveness of 3-TMDs-b is similar to that of a single-TMD, and a reduction effect only occurs between 4-6 s. By contrast, Figure 15 (c) shows that the 5-TMDs system can significantly reduce the vibration amplitudes throughout the event. In terms of reducing slow walking and fast walking-induced vibration, 5-TMDs system exhibits the same effectiveness, as shown in Figure 14. Overall, the vibration reduction capacity of the 5-TMDs system is better than that of single-TMD, 3-TMDs-a, and 3-TMD-b.

The VDV and time history results can be explained by analysing the data in the frequency domain. Figure 16 presents the FFT analysis of the CLT floor free-vibration response without TMD control and with the controls of TMD and MTMD systems. The free vibration acceleration was acquired using heel-drop tests. These show that the vibration of the CLT floor was dominated by one mode at 0-8 Hz when there is no TMD. When the single-TMD was applied, as shown in Figure 16, the first peak of the amplitude in the frequency domain was split into two smaller peaks. According to Den Hartog [30]'s theory, TMD enables the energy in one mode to be distributed into two, and thus the vibration amplitudes in one mode are attenuated. After installing 3-TMDs-a and 3-TMDs-b, the first peak could be split into three and the amplitudes were further reduced. However, the amplitudes at 5.67 Hz using 3-TMD-a and 4.67 Hz using 3-TMD-b were greater than the peak amplitude using a single-TMD. The reason for this is that the designed frequency bandwidth of the 3-TMDs was 4.83-5.57 Hz, as indicated in Table 5, and was thus unable to reduce amplitudes outside this this range. The application of the 5-TMDs offered a wider frequency bandwidth and could lower amplitudes in 4.71-5.69 Hz, as illustrated in Table 5. The 5-TMDs system enabled the amplitudes to be reduced at 4.7-7 Hz; however, the amplitudes around 4.6-4.7 Hz remained larger because they were outside the effective frequency bandwidth of the 5-TMDs. In future MTMD designs for reducing CLT floor vibration, the frequency bandwidth should be designed to cover a broader range.

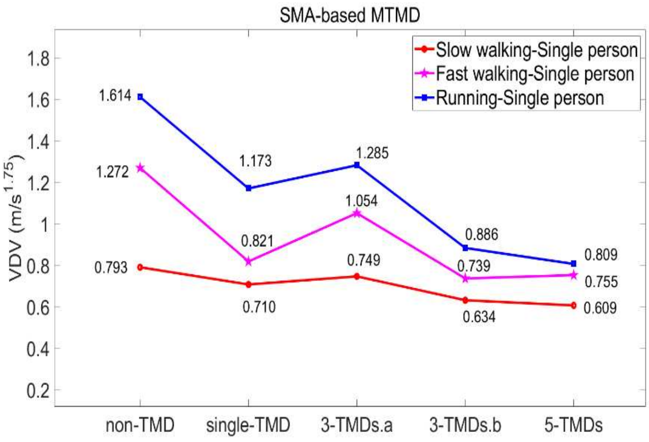

(a)

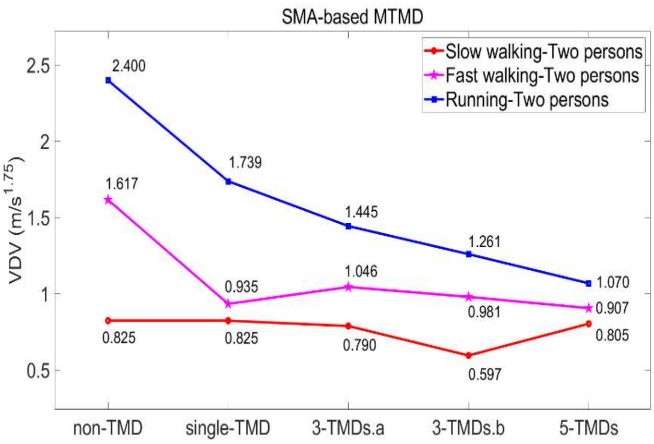

(b)

Figure 14 (a) VDV of the CLT floor with SMA-based TMDs under single-person loadings; (b) VDV of the CLT floor with SMA-based TMDs under two-person loadings

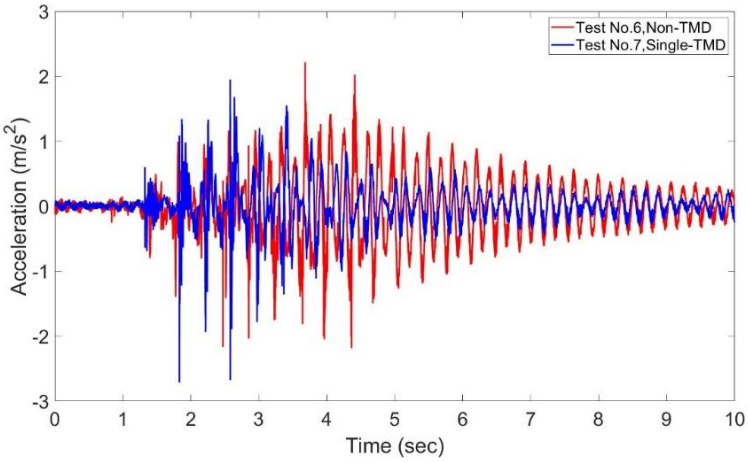

(a)

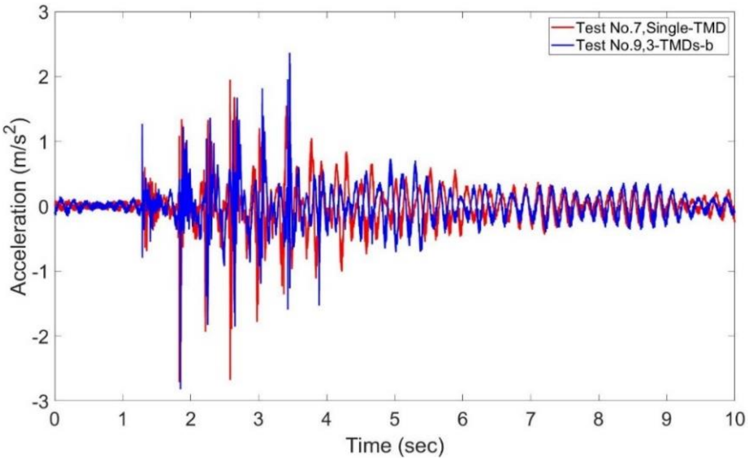

(b)

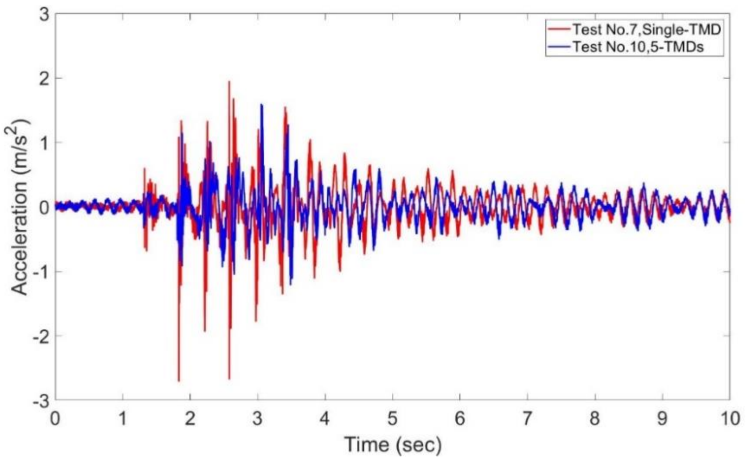

(c)

Figure 15 (a) Time-history under single-person running in Tests Nos. 6 and 7; (a) Time-history under single-person running in Tests Nos. 7 and 9; (c) Time-history under single-person running in Tests Nos.

7 and 10

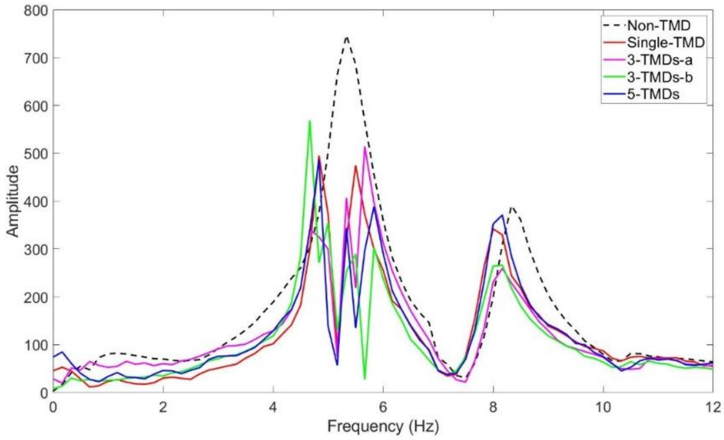

Figure 16 FFT analysis of CLT floor response equipped with different SMA-based MTMD systems

Figure 14 shows that the VDVs of the CLT floor using 3-TMDs-b are smaller than that using 3-TMDs-a. This can be explained by the frequency domain analysis in Figure 16. This shows that the vibration amplitude of the floor using 3-TMDs-b is lower than that using 3-TMDs-a at frequencies of 0-4.1 Hz and 5.3-7.3 Hz. At frequencies higher than 7.3 Hz, the amplitudes are almost identical. Therefore, in most frequency ranges from 0-12 Hz, the amplitude using 3-TMDs-b is lower than that using 3-TMDs-a. However, it is risky if concentrated excitations are between 4.1 and 5.3 Hz on the floor, and the resonance could increase the vibration substantially. To ensure a steady serviceability capacity, an MTMD system with a wider effective bandwidth should be employed such as 5-TMDs.

5.3 Steel-based MTMD systems

Figure 17 presents the VDVs of the CLT floor equipped with steel-based TMD and MTMD systems used in Tests No. 1-5. It shows that the reduction in vibration using a steel-based MTMD is less than that using a SMA-based MTMD. In Figure 17 (a), the VDVs of the CLT floor under single-person running are reduced by only 28% and 25% after applying steel-based 5-TMDs and 3-TMDs-b, respectively, much less than those applying SMA-based 5-TMDs and 3-TMDs-b. The situation is the same under two-person loadings, as presented in Figure 17 (b). Another finding is that the effect of steel-based MTMD is unsatisfactory in reducing the response induced by slow walking.

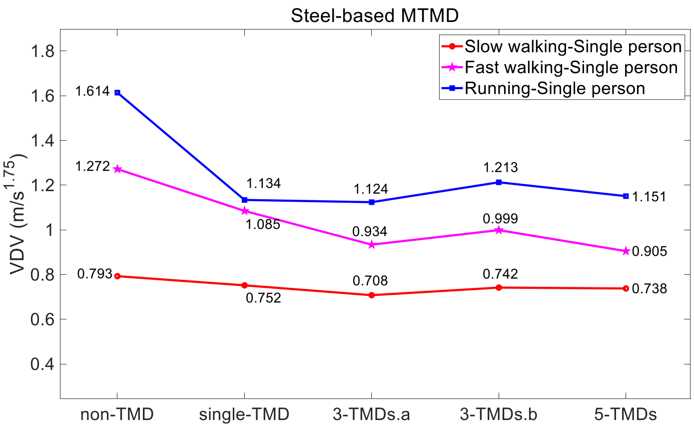

(a)

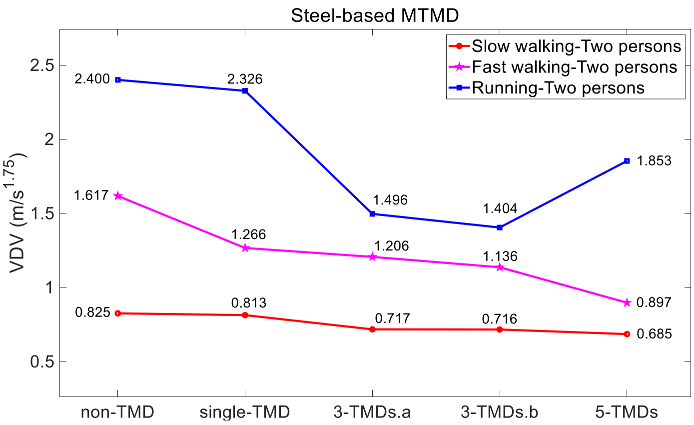

(b)

Figure 17 (a) VDV of the CLT floor with steel-based TMDs under single-person loadings; (b) VDV of the CLT floor with steel-based TMDs under two-person loadings

5.4 Comparison between SMA-based MTMD and steel-based MTMD systems

Figure 18 compares the VDV of the CLT floor equipped with SMA-based MTMD with that equipped with steel-based MTMD. It shows that the VDV using steel-based MTMD is larger than that using SMA-based MTMD in most cases. For example, in Figure 18 (c), the floor response using SMA-based 5-TMDs can be reduced to a low level, and in the vast majority of cases the VDV can be controlled so that it is lower than 1.000 $m/s^{1.75}$.

This is due to the large permanent deformation of the steel bar after two cyclic deformations. During Tests No. 1-5, the bending angle of the steel bars became increasingly larger as the residual strain accumulated. By contrast, no permanent deformation was observed on

SMA bars owing to their superelasticity. The larger bending angle caused by the permanent deformation can lead to a smaller bending moment, which increases the fundamental natural frequency of the TMD. Therefore, the variance of the TMD frequency influences the tuning accuracy. Furthermore, a comparison between SMA and steel bars under cyclic loading in our previous study [34] shows that limited energy is dissipated after the permanent deformation occurs on the steel bar. Variations in the frequency and decreasing of the damping ratio act against optimal tuning with the CLT floor. Therefore, Tests No. 11-15, 21-25, 31-35, and 41-45 were not conducted in further investigations due to miss-tuning of the steel-based TMD and MTMD systems. The additional investigations primarily focused on the performance of the SMA-based TMD and MTMD systems.

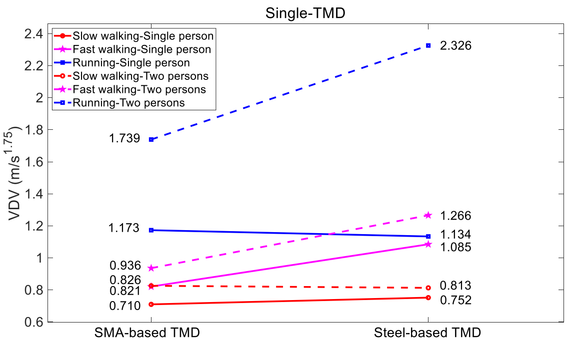

(a)

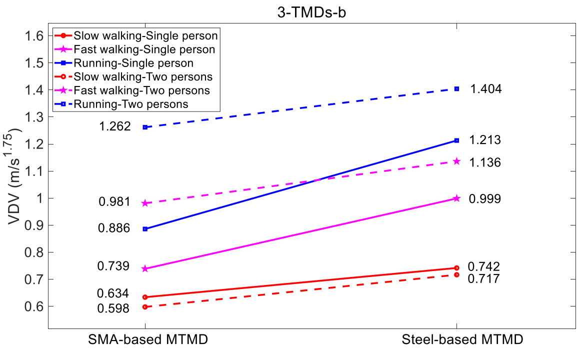

(b)

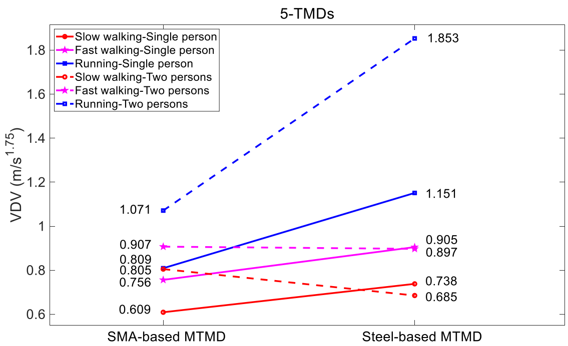

(c)

Figure 18 Comparison of the VDVs (a) between using a SMA-based single TMD and a steel-based single TMD; (b) between using SMA-based 3-TMDs-b and steel-based 3-TMDs-b; (c) between using SMA-based 5-TMDs and steel-based 5-TMDs

5.4 Robustness of the SMA-based MTMD

The investigations presented in Section 5.2 examined the effectiveness of the SMA-based MTMD, and also analysed vibration reduction theories. When dead loadings on the CLT floor are changed, the structural mass can be easily varied and there can be off-tuning problems. The robustness of the MTMD system in adapting to different main structural frequencies must therefore be assessed. Figures 19 and 20 show the VDVs of CLT floor under different loadings (0.08, 0.35, 0.50, 0.65 and 1.50 t) equipped with SMA-based single TMD, 3-TMDs-b, and 5-TMDs. Figure 19 presents the results under the excitation of a single person while Figure 20 presents the results under the excitation of two people. Figure 19 (a) and Figure 20 (a) present the results of Tests No. 7, 17, 27, 37, and 47; Figure 19 (b) and Figure 20 (b) present the results of Tests No. 9, 19, 29, 39, and 49; Figure 19 (c) and Figure 20 (c) present the results of Tests No. 10, 20, 30, 40, and 50.

According to previous studies, increasing the floor mass is conducive to reducing vibration. The VDVs also decrease as the structural mass increased, as shown in Figures 19 and 20. As shown in Figure 19, the VDVs vary greatly with changes in loads when single-TMD and 3-TMDs-b are applied. For instance, in Figure 19 (a), the VDV under fast walking increases from 0.821 $m/s^{1.75}$ to 1.177 $m/s^{1.75}$ (43%) after the loads increase from 0.50 to 0.65 t. Moreover, the VDVs under fast walking increase to 0.908 and 0.955 $m/s^{1.75}$ after the loads decrease to 0.35 and 0.08 t, respectively. As presented in Figure 19 (b), the variance of the VDVs as the loads change is also large when the 3-TMDs-b system is equipped, especially under running. When the 5-TMDs system is employed, the VDVs can be reduced to a lower level and remain constant with changing loads, as shown in Figure 19 (c). Table 7 presents the standard deviation (SD) of the VDVs and the averaged VDVs over different loads in each testing condition. This shows that the SD of VDVs and the averaged VDVs under single-person excitations can be controlled to a low level when the 5-TMDs system is employed. This means that the variation of VDVs is small over different loadings and the 5-TMDs system is robust enough to adapt to different loading conditions.

As presented in Figure 20, the VDVs under two-person walking maintain a steady downward trend as the loads increase with a 5-TMDs system, contrasting with those of single-TMD and 3-TMDs. Table 7 shows that the SD of VDVs and the averaged VDVs with 5-TMDs are reduced to a small level. However, the SD of VDVs under running with 5-TMDs is larger than those under slow and fast walking due to a big drop from 1.479 to 1.071 $m/s^{1.75}$ (Figure 20 (c)). It is important to note that there were fluctuations in the VDVs with changing loads under two-person running in single-TMD, 3-TMDs, and 5-TMDs equipment conditions. Because running induces heel strike and toe-lift off of the floor, it can exert high-frequency loadings, as indicated in [11]. When two persons ran simultaneously, the excitation contained high-frequency loadings at 2.2, 4.4, 6.7 and even 8.9 Hz, much higher than the effective bandwidth of the 5-TMDs system.

In summary, the 5-TMDs system has been shown to have high robustness over different loading conditions. The VDVs of the CLT floor with the application of 5-TMDs can be controlled to a low level. However, the effectiveness of the 5-TMDs system is degraded when the excitations contain high-frequency loadings. Future MTMD systems should be designed to possess a broader bandwidth.

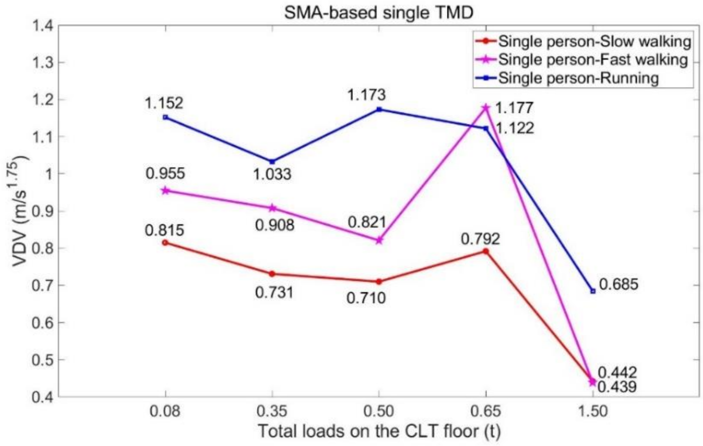

(a)

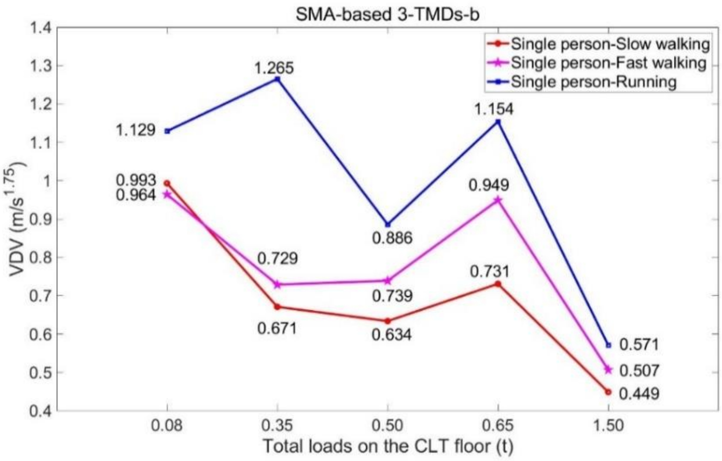

(b)

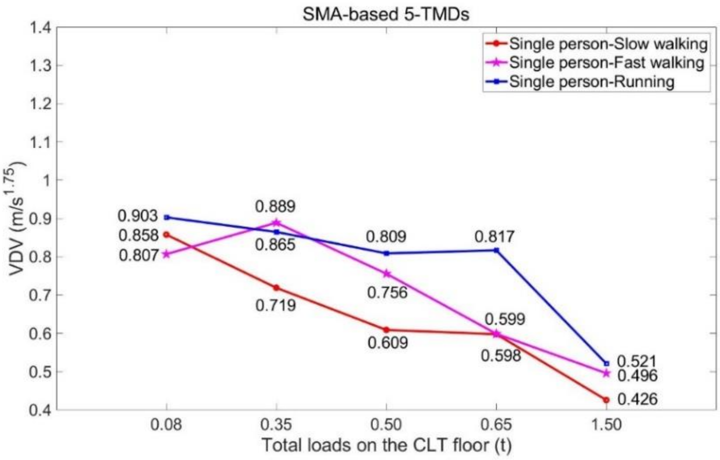

(c)

Figure 19 (a) Single-person-induced VDVs of the CLT floor with SMA-based single TMD under different loads; (b) Single-person-induced VDVs of the CLT floor with SMA-based 3-TMDs-b under different loads; (c) Single-person-induced VDVs of the CLT floor with SMA-based 5-TMDs under different loads;

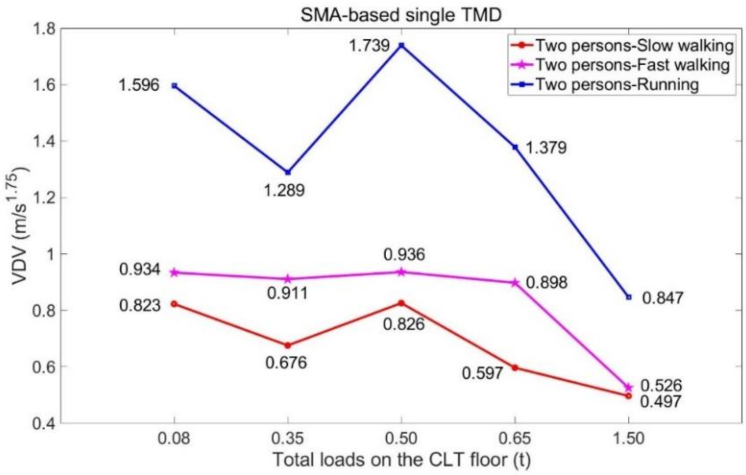

(a)

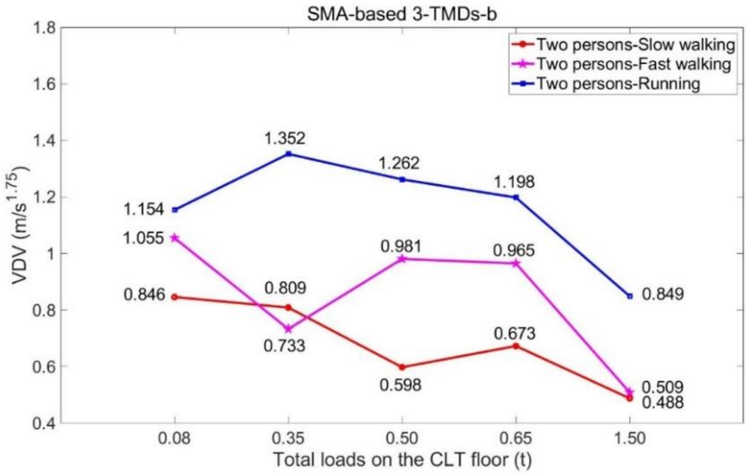

(b)

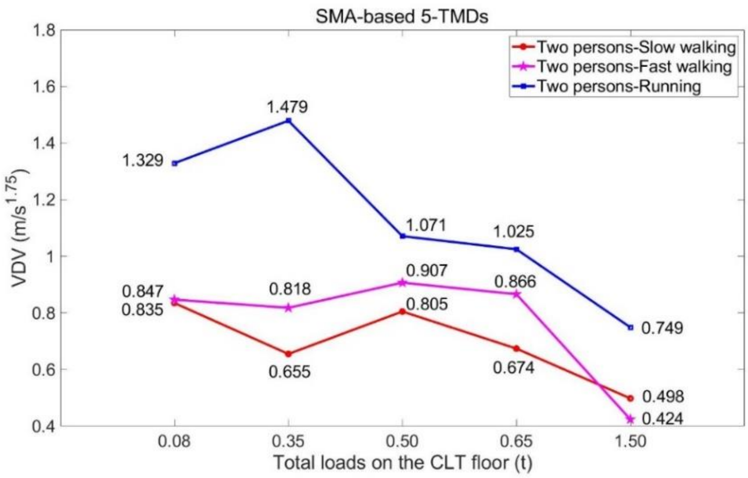

(c)

Figure 20 (a) Two-person-induced VDVs of the CLT floor with SMA-based single TMD under different loads; (b) Two-person-induced VDVs of the CLT floor with SMA-based 3-TMDs-b under different loads; (c) Two-person-induced VDVs of the CLT floor with SMA-based 5-TMDs under different loads;

Table 7 Standard derivation of VDVs and averaged VDVs over different loads in each testing condition

		Single-TMD	3TMDs-b	5TMDs
Single-person slow walking	Standard derivation	0.134	0.176	0.143
	Averaged VDV ($m/s^{1.75}$)	0.698	0.695	0.642
Single-person fast walking	Standard derivation	0.241	0.168	0.143
	Averaged VDV ($m/s^{1.75}$)	0.860	0.778	0.709
Single-person running	Standard derivation	0.180	0.248	0.135
	Averaged VDV ($m/s^{1.75}$)	1.033	1.001	0.783
Two-person slow walking	Standard derivation	0.128	0.133	0.120
	Averaged VDV ($m/s^{1.75}$)	0.684	0.683	0.693
Two-person fast walking	Standard derivation	0.158	0.201	0.177
	Averaged VDV ($m/s^{1.75}$)	0.841	0.849	0.772
Two-person running	Standard derivation	0.306	0.171	0.253
	Averaged VDV ($m/s^{1.75}$)	1.370	1.163	1.130

6. Conclusions

Through a series of experimental tests, this study investigated the effectiveness of steel-based and SMA-based MTMD systems on reducing the vibration of a CLT floor. The MTMD systems were designed to be effective in a bandwidth to overcome off-tuning problems. The testing results were analysed using the VDV method which was calculated by weighted accelerations. Based on the results, the following conclusions can be drawn:

- The SMA-based MTMD system was able to reduce human-induced vibration such as single/two-person slow walking, fast walking, and running.
- The SMA-based 5-TMDs system was shown to be the most effective as it reduced the VDV by about 50%.
- The effectiveness of the steel-based MTMD was unsatisfactory in comparison with SMA-based MTMD due to the accumulated permanent deformation that was observed.
- The SMA-based 5-TMDs system was the most robust as the floor response remained steady over different loadings.

Thus, the use of SMA-based 5-TMDs as a passive control strategy is suitable for CLT floor vibration control. In future, a MTMD with a wider bandwidth should be developed for CLT floors to achieve higher robustness.

Acknowledgement

The authors would like to thank the financial support from National Natural Science Foundation of China (51908007), Beijing Municipal Education Commission (KM201910005021) and Basic Research Foundation of Beijing University of Technology.

Reference:

1. Standardization, E.C.f., *EN 1995-1-1:2004+A2. Eurocode 5: Design of timber structures–Part 1-1: General–Common rules and rules for buildings.* 2014: Brussels (Belgium).
2. (FHA), F.H.A., *Minimum property standards for one ad two living units.* 1964: Washington, DC.
3. Canada, N.r.C.o., *National Building Code of Canada Appendix A: Explanatory material for the national Building Code.* 1990: Ottawa.
4. Setareh, M. and D. Hanson Robert, *Tuned Mass Dampers to Control Floor Vibration from Humans.* Journal of Structural Engineering, 1992. **118**(3): p. 741-762.
5. Webster, A.C. and R. Vaicaitis, *Application of Tuned Mass Dampers To Control Vibrations of Composite Floor Systems.* Journal of the American Institute of Steel Construction, 1992. **Third Quarter**: p. 116-124.
6. Setareh, M., et al., *Pendulum Tuned Mass Dampers for Floor Vibration Control.* Journal of Performance of Constructed Facilities, 2006. **20**(1): p. 64-73.
7. Santos, M.D.S.d., et al., *Vibration control of a gym floor using tuned mass dampers: a numerical analysis.* Modern Mechanical Engineering, 2013. **3**: p. 9-16.
8. Nguyen, T.H., et al., *Performance of Distributed Multiple Viscoelastic Tuned Mass Dampers for Floor Vibration Applications.* Advances in Structural Engineering, 2012. **15**(3): p. 547-562.
9. Chang, M.-L., et al., *Experimental study on adjustable tuned mass damper to reduce floor vibration due to machinery.* Structural Control and Health Monitoring, 2010. **17**(5): p. 532-548.
10. Wang, X., et al., *A general vibration control methodology for human-induced vibrations.* Structural Control and Health Monitoring, 2019. **26**(10): p. e2406.
11. Huang, H. and W.-S. Chang, *Application of pre-stressed SMA-based tuned mass damper to a timber floor system.* Engineering Structures 2018. **167**: p. 143-150.
12. Setareh, M., *Floor vibration control using semi-active tuned mass dampers.* Canadian Journal of Civil Engineering, 2002. **29**(1): p. 76-84.
13. Setareh, M., et al., *Semiactive Tuned Mass Damper for Floor Vibration Control.* Journal of Structural Engineering, 2007. **133**(2): p. 242-250.
14. Huang, H.Y., W.S. Chang, and K.M. Mosalam, *Feasibility of shape memory alloy in a tuneable mass damper to reduce excessive in-service vibration.* Structural Control & Health Monitoring, 2017. **24**(2): p. 1-14.
15. Rahmani, H.R. and C. Konke, *Seismic Control of Tall Buildings Using Distributed Multiple Tuned Mass Dampers.* Advances in Civil Engineering, 2019: p. 1-19.

16. Yamaguchi, H. and N. Harnpornchai, *Fundamental characteristics of Multiple Tuned Mass Dampers for suppressing harmonically forced oscillations.* Earthquake Engineering & Structural Dynamics, 1993. **22**(1): p. 51-62.
17. Dehghan-Niri, E., S.M. Zahrai, and A. Mohtat, *Effectiveness-robustness objectives in MTMD system design: An evolutionary optimal design methodology.* Structural Control and Health Monitoring, 2010. **17**(2): p. 218-236.
18. Lin, P.Y., L.L. Chung, and C.H. Loh, *Semiactive control of building structures with semiactive tuned mass damper.* Comput-Aided Civ Inf, 2005. **20**(1): p. 35-51.
19. Varadarajan, N. and S. Nagarajaiah, *Wind response control of building with variable stiffness tuned mass damper using empirical mode decomposition/Hilbert transform.* Journal of Engineering Mechanics-Asce, 2004. **130**(4): p. 451-458.
20. Wang, L., et al., *Study on adaptive-passive multiple tuned mass damper with variable mass for a large-span floor structure.* Engineering Structures, 2020. **209**: p. 110010.
21. Duerig, T.W., *Engineering aspects of shape memory alloys*. 1990, London ; Boston: Butterworth-Heinemann. xi, 499 p.
22. Huang, H., Y.-Z. Zhu, and W.-S. Chang, *Comparison of Bending Fatigue of NiTi and CuAlMn Shape Memory Alloy Bars.* Advances in Materials Science and Engineering, 2020. **2020**: p. 1-9.
23. Huang, H.Y. and W.S. Chang, *Seismic resilience timber connectionadoption of shape memory alloy tubes as dowels.* Structural Control & Health Monitoring, 2017. **24**(10).
24. Chang, W.-S. and Y. Araki, *Use of shape memory alloy in construction: A critical review.* Proceedings of the ICE - Civil Engineering, 2016.
25. Committee, C.N.S.M., *Hot rolled H and cut T section steel (GB/T 11263-2017)*. 2017, China Standards Press: Beijing.
26. Committee, C.N.S.M., *Carbon sructural steels (GB/T 700-2006)*. 2006, China Standards Press: Beijing.
27. Sarkar, T.K. and O. Pereira, *Using the Matrix Pencil Method to Estimate the Parameters of a Sum of Complex Exponentials.* Ieee Antennas and Propagation Magazine, 1995. **37**(1): p. 48-55.
28. Zieliński, T.P. and K. Duda, *Frequency and damping estimation methods - an overview.* Metrology and measurement systems, 2011. **18**(4): p. 505 - 528.
29. Committee, C.N.S.M., *Cold rolled stainless steel plate, sheet and strip (GB/T 3280-2015)*. 2015, China Standards Press: Beijing.
30. Den Hartog, J.P., *Mechanical vibrations*. 4th ed. 1956, New York ; London: McGraw-Hill. xi, 436 p.
31. Wang, C. and W.X. Shi, *Optimal Design and Application of a Multiple Tuned Mass Damper System for an In-Service Footbridge.* Sustainability, 2019. **11**(10).
32. BSI, *BS 6472-1:2008. British standard. Guide to evaluation of human exposure to vibration in buildings – Part 1: Vibration sources other than blasting*. 2008: London, UK.
33. (ISO), I.S.O., *ISO 10137: Bases for design of structures – serviceability of buildings and walkways against vibrations*. 2007: Geneva.
34. Chang, W.S., et al., *Technical Note: Potential to Use Shape Memory Alloy in Timber Dowel-Type Connections.* Wood and Fiber Science, 2013. **45**(3): p. 330-334.